

PREPARED FOR SUBMISSION TO JHEP

Triple Higgs Boson Production with Two Heavy Scalars at the LHC via a Simplified Approach

Andreas Papaefstathiou,¹ Gilberto Tetlalmatzi-Xolocotzi,²

¹*Department of Physics, Kennesaw State University, 830 Polytechnic Lane, Marietta, GA 30060, USA*

²*Theoretische Physik 1, Center for Particle Physics Siegen (CPPS), Universität Siegen, Walter-Flex-Str. 3, 57068 Siegen, Germany*

E-mail: apapaefs@kennesaw.edu, gtx@physik.uni-siegen.de

ABSTRACT: We investigate triple Higgs boson production at the CERN LHC, in models containing two new neutral scalar particles heavier than the Higgs boson. We apply a simplified factorized approach in the narrow-width approximation to double-resonant triple Higgs boson production, and demonstrate that relevant constraints can be derived on models with extended scalar sectors, during the high-luminosity phase of the LHC. We also show that analyzing the double-resonant process will be sufficient at the LHC, within an explicit model with two real singlet scalar fields, and that non-resonant components are not expected to play a crucial role in the specific scenario. The method can be applied to any model where triple Higgs boson production can be enhanced via the double-resonant process in the presence of two new neutral scalar resonances.

Contents

1	Introduction	1
2	Extending the Standard Model by Real Singlet Scalar Fields	2
3	A Simplified Approach to Double-Resonant Triple Higgs Boson Production	4
4	Phenomenological Analysis at the LHC	9
4.1	Limits on the (m_2, m_3) -plane	9
4.2	Case Studies: Resonant Versus Full Non-Resonant Production at the LHC	14
5	Conclusions	16

1 Introduction

Multi-Higgs boson production processes at colliders, such as the CERN Large Hadron Collider (LHC), can provide further insight into the electroweak and scalar sectors of the standard model (SM), going beyond the information harnessed by the discovery [1, 2] of the Higgs boson [3–5] itself. The two primary multi-Higgs boson production processes, pair production and triple production, can be used within the SM to yield a consistency check of the triple and quartic self-interactions, respectively, verifying the “standard” shape of the Higgs boson’s (h_1) potential,

$$\mathcal{V}(h_1) = \frac{1}{2}m_{h_1}^2 h_1^2 + \frac{m_{h_1}^2}{2v} h_1^3 + \frac{m_{h_1}^2}{8v^2} h_1^4, \quad (1.1)$$

where $m_{h_1} \approx 125$ GeV is the Higgs boson mass, and $v \approx 246$ GeV is the Higgs vacuum expectation value. In the realm of such self-coupling measurements, within and beyond the SM, Higgs boson pair production has received considerable attention through experimental (e.g. [6–35]) and theoretical (e.g. [36–97]) studies. Primarily due to its tiny SM cross section at hadron colliders [62], the triple Higgs boson process has received much less attention. To the extent of our knowledge, it was first investigated in [98], where it was demonstrated that the prospects for the measurement of the quartic self-coupling will be very challenging, both at the LHC and at a future ‘VLHC’, with a center-of-mass energy of 200 TeV. Subsequent studies of triple Higgs boson production at future colliders [99–108], with the knowledge of the value of the Higgs boson mass, and the prospects for Higgs boson pair production measurements at hand, further quantified the difficulty of this measurement, nevertheless demonstrating that *some* useful information may be obtained via the process.

At LHC energies, the situation for triple Higgs boson production is much more dire, as expected, requiring either new phenomena for sufficient enhancement [109–111], or very

large new anomalous contributions, either to the Higgs boson’s self-interactions [112, 113], or to the Higgs-heavy quark or Higgs-gluon interactions [113]. More specifically, in the context of explicit models of new physics, it has been shown, within the two-real singlet model (TRSM), that triple Higgs boson production may be enhanced to a level sufficient for observation and exploration at the LHC [109–111]. This is possible through the opening of the double-resonant process $gg \rightarrow h_3 \rightarrow (h_2 \rightarrow h_1 h_1) h_1$ when $m_3 > m_2 + m_1$ and $m_2 > 2m_1$, where h_1 is the SM-like Higgs boson, and h_2 and h_3 are two new heavy scalar particles (see fig. 1 below), as first proposed in [109], investigated further in [110, 111], and in the recent experimental study including the first-ever results on triple Higgs boson searches by the ATLAS collaboration [114]. Additionally, due to current constraints on the production rates of new scalar particles which mix with the SM-like Higgs boson, the widths of the h_2 and h_3 are expected to be generically small, $\mathcal{O}(1 \text{ GeV})$, enforcing the validity of the narrow width approximation for this process. Therefore, the double-resonant process can be factorized at each step to a good approximation, leading to substantial simplifications to its phenomenological treatment. In this paper, we demonstrate these simplifications, providing a simple phenomenological analysis, and deriving constraints that can be applied to *any* model with extended scalar sectors that may be capable of producing this process. Within this framework we examine the prospect for detecting the example benchmark parameter-space points within the TRSM, generated following the treatment of ref. [111]. With the developed analysis, we examine and contrast the effect of the non-resonant part of the process in explicit case studies within the TRSM.

The paper is organized as follows: in section 2 we discuss extended scalar sectors, outlining some of the properties of our the case study model, the TRSM. In section 3 we discuss the simplified approach to the phenomenology of this process, and in section 4 we perform an analysis for the LHC over the allowed range of masses for the processes, as well as a case study examining the effects of the non-resonant parts. We present our conclusions in section 5.

2 Extending the Standard Model by Real Singlet Scalar Fields

The scalar potential of the SM can be extended by an additional sector of scalar fields. These can transform as singlets, doublets, triplets and so on. For the sake of simplicity, we focus on the case that the new fields transform as singlets under the SM gauge group, leading to

$$\mathcal{V}(\Phi, \phi_i) = \mathcal{V}_{\text{singlets}}(\Phi, \phi_i) + \mathcal{V}_{\text{SM}}(\Phi), \quad (2.1)$$

with the most general renormalizable expression for $\mathcal{V}_{\text{singlets}}(\Phi, \phi_i)$ given by

$$\begin{aligned} \mathcal{V}_{\text{singlets}}(\Phi, \phi_i) = & a_i \phi_i + m_{ij} \phi_i \phi_j + \tilde{\lambda}_{ijk} \phi_i \phi_j \phi_k + \tilde{\lambda}_{ijkl} \phi_i \phi_j \phi_k \phi_l \\ & + \tilde{\kappa}_{iHH} \phi_i (\Phi^\dagger \Phi) + \tilde{\kappa}_{ijHH} \phi_i \phi_j (\Phi^\dagger \Phi). \end{aligned} \quad (2.2)$$

The goal of the present paper is to study enhanced triple Higgs boson production at the LHC in models that contain at least two additional physical scalar particles, beyond the

SM-like Higgs boson, and the methods developed herein could also be applied to non-singlet scalar extensions of the SM scalar sector. As a particular example of such a model, we will use the TRSM [109–111], where two extra real scalar singlet fields S and X are introduced. To reduce the number of free parameters, the following discrete \mathbb{Z}_2 symmetries are imposed:

$$\begin{aligned}\mathbb{Z}_2^S &: S \rightarrow -S, \quad X \rightarrow X, \\ \mathbb{Z}_2^X &: X \rightarrow -X, \quad S \rightarrow S,\end{aligned}\tag{2.3}$$

with all SM particles transforming evenly under both symmetries. The application of the discrete symmetries of eq. 2.3 reduces the scalar potential for two real singlet fields to:

$$\begin{aligned}\mathcal{V}(\Phi, X, S) &= \mu_\Phi^2 \Phi^\dagger \Phi + \lambda_\Phi (\Phi^\dagger \Phi)^2 + \mu_S^2 S^2 + \lambda_S S^4 + \mu_X^2 X^2 + \lambda_X X^4 \\ &+ \lambda_{\Phi S} \Phi^\dagger \Phi S^2 + \lambda_{\Phi X} \Phi^\dagger \Phi X^2 + \lambda_{SX} S^2 X^2,\end{aligned}\tag{2.4}$$

which is characterized by nine real free couplings μ_Φ , λ_Φ , μ_S , λ_S , μ_X , λ_X , $\lambda_{\Phi S}$, $\lambda_{\Phi X}$, λ_{SX} . All fields are assumed to acquire a vacuum expectation value (vev). The physical gauge-eigenstates $\phi_{h,S,X}$ then follow from expanding around these according to:

$$\Phi = \begin{pmatrix} 0 \\ \frac{\phi_h + v}{\sqrt{2}} \end{pmatrix}, \quad S = \frac{\phi_S + v_S}{\sqrt{2}}, \quad X = \frac{\phi_X + v_X}{\sqrt{2}}.\tag{2.5}$$

We will work in the broken phase in which, generically, $v_S, v_X \neq 0$ and $v = v_{\text{SM}} \simeq 246$ GeV. Then, the discrete symmetries \mathbb{Z}_2^S and \mathbb{Z}_2^X are spontaneously broken and the scalars ϕ_h , ϕ_S , ϕ_X mix into the physical states h_1 , h_2 and h_3 according to the rotation:

$$\begin{pmatrix} h_1 \\ h_2 \\ h_3 \end{pmatrix} = R \begin{pmatrix} \phi_h \\ \phi_S \\ \phi_X \end{pmatrix},\tag{2.6}$$

with the rotation matrix R given by

$$R = \begin{pmatrix} c_1 c_2 & -s_1 c_2 & -s_2 \\ s_1 c_3 - c_1 s_2 s_3 & c_1 c_3 + s_1 s_2 s_3 & -c_2 s_3 \\ c_1 s_2 c_3 + s_1 s_3 & c_1 s_3 - s_1 s_2 c_3 & c_2 c_3 \end{pmatrix},\tag{2.7}$$

where we have used as shorthand:

$$\begin{aligned}s_1 &\equiv \sin \theta_{12}, & s_2 &\equiv \sin \theta_{13}, & s_3 &\equiv \sin \theta_{23}, \\ c_1 &\equiv \cos \theta_{12}, & c_2 &\equiv \cos \theta_{13}, & c_3 &\equiv \cos \theta_{23},\end{aligned}\tag{2.8}$$

with the mixing angles within the range:

$$-\frac{\pi}{2} < \theta_{12}, \theta_{13}, \theta_{23} < \frac{\pi}{2}.\tag{2.9}$$

Using the same notation as in [109, 110], the entries of the first row in the matrix R are denoted as $\kappa_i \equiv R_{i1}$ for $i = 1, 2, 3$. The h_1 state can be identified with the SM-like Higgs boson, and h_2 and h_3 are two new physical *heavier* scalars obeying the mass hierarchy

$$m_1 \leq m_2 \leq m_3.\tag{2.10}$$

There are *nine* real parameters that characterize the TRSM. However, the identification of h_1 as the SM Higgs boson fixes

$$\begin{aligned} m_1 &\simeq 125 \text{ GeV}, \\ v &\simeq 246 \text{ GeV}. \end{aligned} \tag{2.11}$$

This leaves us with seven independent parameters, which can be chosen to be:

$$m_2, m_3, \theta_{12}, \theta_{13}, \theta_{23}, v_2, v_3. \tag{2.12}$$

In this model all couplings for the mass eigenstates h_i to SM particles are inherited from the SM-like Higgs doublet through the rotation from the gauge to the mass eigenstates, such that their couplings are rescaled with respect to the SM Higgs boson couplings by a mixing factor κ_i : $g_i \equiv \kappa_i g^{\text{SM}}$. For example, in a factorized approach, this leads to predictions for production cross sections of the form

$$\sigma(pp \rightarrow h_i) = \kappa_i^2 \sigma^{\text{SM}}(pp \rightarrow h_{\text{SM}})(m_i), \tag{2.13}$$

where $\sigma^{\text{SM}}(m_i)$ denotes the production cross section of an SM-like Higgs boson of mass m_i . Furthermore, the total width of the h_i scalars ($i = 1, 2, 3$) is given by:

$$\Gamma_{h_i} = \kappa_i^2 \Gamma^{\text{SM}}(m_i) + \sum_{j,k,(l) \neq i} \Gamma_{h_i \rightarrow h_j h_k (h_l)}, \tag{2.14}$$

where $\Gamma^{\text{SM}}(m_i)$ corresponds to the width of a scalar boson of mass m_i possessing the same decay modes as a SM Higgs boson of mass m_i . The branching ratios corresponding to $h_i \rightarrow xx$, for $x \neq h_j$ ($j \neq i$) are then given by:

$$\text{BR}(h_i \rightarrow xx) = \kappa_i^2 \frac{\Gamma_{xx}^{\text{SM}}(m_i)}{\Gamma_{h_i}}, \tag{2.15}$$

where $\Gamma_{xx}^{\text{SM}}(m_i)$ corresponds to the SM-like partial decay width of a scalar boson of mass M_i for the final state xx . The scalar-to-scalar branching ratios are equivalently obtained via

$$\text{BR}(h_i \rightarrow h_j h_k (h_l)) = \frac{\Gamma_{h_i \rightarrow h_j h_k (h_l)}}{\Gamma_{h_i}}. \tag{2.16}$$

The triple couplings between scalars ijk have been derived in [109], and the quartic couplings between scalars $ijkl$ have been derived in [110], both in terms of the parameters of eq. 2.12.

3 A Simplified Approach to Double-Resonant Triple Higgs Boson Production

In the present study, we focus on the largest enhancement in triple Higgs boson production via gluon fusion, i.e. $pp \rightarrow h_1 h_1 h_1$, coming through the double-resonant production $gg \rightarrow$

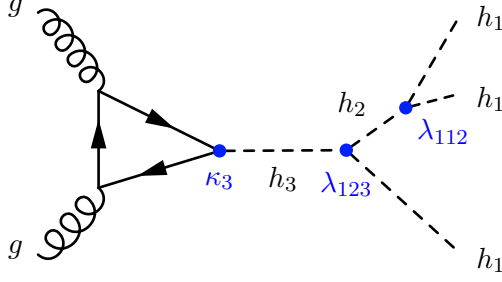


Figure 1: Double-resonant triple SM-like Higgs boson (h_1) production in a model with two heavy scalars h_3 and h_2 , with $m_3 > m_2 + m_1$.

$h_3 \rightarrow (h_2 \rightarrow h_1 h_1) h_1$, in a model where the masses of the three scalars satisfy $m_3 > m_2 + m_1$ and $m_2 > 2m_1$, such that all particles are produced on-shell, see fig. 1. In this case, the cross section corresponding to this process can be written as:

$$\sigma(m_2, m_3) = \sigma_u(m_2, m_3) \times \kappa_3^2 \lambda_{123}^2 \lambda_{112}^2, \quad (3.1)$$

where $\sigma_u(m_2, m_3)$ is the cross section for the process when the κ_3 parameter is set to unity, and the couplings λ_{123} and λ_{112} are set to 1 GeV. Furthermore, if we assume that h_2 and h_3 have narrow widths, such that $\Gamma_i \ll M_i$, then they are both produced near on-shell, and we can replace the related Breit-Wigner factors in the cross section by δ -functions via the standard substitution:¹

$$\frac{dq_i^2}{(q_i^2 - m_i^2)^2 + m_i^2 \Gamma_i^2} \rightarrow \frac{\pi}{m_i \Gamma_i} \delta(q_i^2 - m_i^2) dq_i^2 \quad (3.3)$$

With the substitution of eq. 3.3, we can then write the cross section for the double-resonant production as follows:

$$\begin{aligned} \sigma(m_2, m_3, \Gamma_2, \Gamma_3, \kappa_3, \lambda_{123}, \lambda_{112}) &= \hat{\sigma}_u(m_2, m_3) \times \frac{\kappa_3^2 \lambda_{123}^2 \lambda_{112}^2}{\Gamma_2 \Gamma_3} \\ &= \hat{\sigma}_u(m_2, m_3) \times \rho^2, \end{aligned} \quad (3.4)$$

where now $\hat{\sigma}_u(m_2, m_3)$ is the cross section for the process for $\kappa_3 = 1$, $\lambda_{123} = \lambda_{112} = 1$ GeV, and $\Gamma_2 = \Gamma_3 = 1$ GeV, and the second line defines the rescaling factor

$$\rho^2 \equiv \kappa_3^2 \lambda_{123}^2 \lambda_{112}^2 / (\Gamma_2 \Gamma_3). \quad (3.5)$$

We call $\hat{\sigma}_u(m_2, m_3)$ the ‘unity’ cross section for brevity. The rescaling factor ρ^2 is given for the selected subset of benchmark points derived in ref. [111], which we reproduce in table 1, along with their defining parameters: the masses m_2 , m_3 , the vacuum expectation values

¹This can be derived by considering the integral of the Breit-Wigner factor over the virtuality of the particle, q_i^2 , as follows (see, e.g. [115]):

$$\int_{-\infty}^{+\infty} \frac{dq_i^2}{(q_i^2 - m_i^2)^2 + m_i^2 \Gamma_i^2} = \frac{\pi}{m_i \Gamma_i}. \quad (3.2)$$

Benchmark info for enhanced triple Higgs production from ref. [111]									
Name	m_2	m_3	v_2	v_3	θ_{12}	θ_{13}	θ_{23}	$\frac{\sigma}{\sigma_{SM}}$	R.F.
BM0	259.0	495.0	215.8	180.8	6.191	0.1629	5.691	306.0	0.9552
BM1	270.6	444.7	122.4	847.2	0.268	0.030	0.522	302.4	0.929
BM2	268.6	452.7	137.8	784.8	0.2632	0.023	0.645	275.6	0.9536
BM3	272.6	480.7	928.3	143.7	3.098	2.9	2.38	267.2	0.9476
BM4	269.0	409.8	138.0	599.4	0.2436	0.004	0.773	266.4	0.9761
BM5	269.1	486.9	227.5	307.9	0.074	6.149	2.631	157.6	0.9557
BM6	259.2	577.0	289.0	275.6	0.137	6.148	2.324	145.5	0.781
BM7	283.7	575.0	259.4	330.4	0.137	6.152	2.299	122.5	0.7791
BM8	264.3	469.3	207.3	359.5	0.2847	6.277	0.692	119.1	0.9988
BM9	266.5	461.9	653.1	229.0	2.889	3.046	1.015	112.8	0.8632
BM10	259.2	399.7	444.5	217.0	2.917	3.046	1.047	103.7	0.973

Table 1: A sample of selected benchmark points obtained during the scan of ref. [111] for the TRSM. The masses m_2 , m_3 , and the vacuum expectation values v_2 and v_3 are given in GeV. The three mixing angles θ_{12} , θ_{13} and θ_{23} are also provided. The second from last column indicates the enhancement factor over the expected SM value at the 13.6 TeV LHC. The last column shows the fraction of the resonant double-resonant contribution to the total cross section for triple Higgs boson production, labeled in shorthand as “R.F.”. A complete list is provided in the ancillary files of ref. [111].

v_2 and v_3 (in GeV), and the three mixing angles θ_{12} , θ_{13} and θ_{23} . We note that this value of ρ^2 represents a leading-order calculation. Higher-order corrections can be applied via a k -factor, by calculating them for the case of on-shell h_3 production, i.e. $(\rho^2)^{\text{HO}} = k_{\text{fac}} \times (\rho^2)^{\text{LO}}$, where $(\rho^2)^{\text{HO}}$ is the higher-order rescaling factor. In the present article, we opt for the simple choice of $k_{\text{fac}} = 2$ for all signal processes. The enhancement factors over the expected, non-resonant SM triple Higgs boson production at a 13.6 TeV LHC, and the resonant fraction (R.F.), corresponding to the approximate contribution of the double-resonant process to the total cross section are also given in table 1. Table 2 shows, for the same benchmarks, the parameters relevant to double-resonant triple Higgs boson production: m_2 , m_3 , Γ_2 , Γ_3 , κ_3 , λ_{123} and λ_{112} , as well as the rescaling factor, ρ^2 , as defined by eq. 3.4, and the unity cross section for the given combination of masses, $\hat{\sigma}_u(m_2, m_3)$. We show a contour plot of the unity cross section, $\hat{\sigma}_u$, in fig. 3 for proton collisions at a 13.6 TeV LHC. The region $m_3 < m_2 + m_1$ is excluded since the double-resonant process is zero by definition there, as it is kinematically disallowed.

Therefore, the on-shell simplifications of the double-resonant process suggest the following approach: one can perform a phenomenological analysis on Monte Carlo event samples with $\kappa_3 = 1$, $\lambda_{123} = \lambda_{112} = 1$ GeV, and $\Gamma_2 = \Gamma_3 = 1$ GeV, and obtain the constraint for

Benchmark quantities relevant for double-resonant triple Higgs boson production

Name	m_2	m_3	Γ_2	Γ_3	κ_3	λ_{123}	λ_{112}	ρ^2 [$\times 10^6$]	$\hat{\sigma}_u$ [$\times 10^{-9}$]
BM0	259.0	495.0	0.003514	3.927	0.1854	-191.8	8.167	6.11	2.018
BM1	270.6	444.7	0.5078	2.586	0.1571	-204.3	67.52	3.574	3.408
BM2	268.6	452.7	0.3805	3.142	0.1741	-203.6	57.78	3.509	3.165
BM3	272.6	480.7	0.2009	4.758	0.2024	-224.6	41.39	3.703	2.908
BM4	269.0	409.8	0.2836	1.995	0.1713	-180.3	48.89	4.031	2.663
BM5	269.1	486.9	0.0003346	2.017	0.1527	103.3	-2.477	2.264	2.805
BM6	259.2	577.0	0.0006274	5.79	0.1908	196.3	-3.701	5.289	1.108
BM7	283.7	575.0	0.001056	5.587	0.1884	193.5	-3.578	2.885	1.711
BM8	264.3	469.3	0.3916	2.941	0.1746	-144.3	55.88	1.721	2.789
BM9	266.5	461.9	0.3092	2.042	0.1635	142.8	39.98	1.381	3.29
BM10	259.2	399.7	0.2188	0.9312	0.1463	121.2	35.41	1.936	2.159

Table 2: A sample of selected benchmark points obtained during the scan of ref. [111] for the TRSM. The particle masses m_2 , m_3 , and the widths Γ_2 and Γ_3 are given in GeV. The h_3 rescaling factor, κ_3 , and the $h_1 - h_2 - h_3$ and $h_1 - h_1 - h_2$ scalar couplings (in GeV) are also given. The second-to-last column indicates the leading-order rescaling factor ρ^2 in GeV^2 , as defined by eq. 3.4. The last column represents the unity cross section for the given combination of masses, $\hat{\sigma}_u(m_2, m_3)$, in pb/GeV^2 .

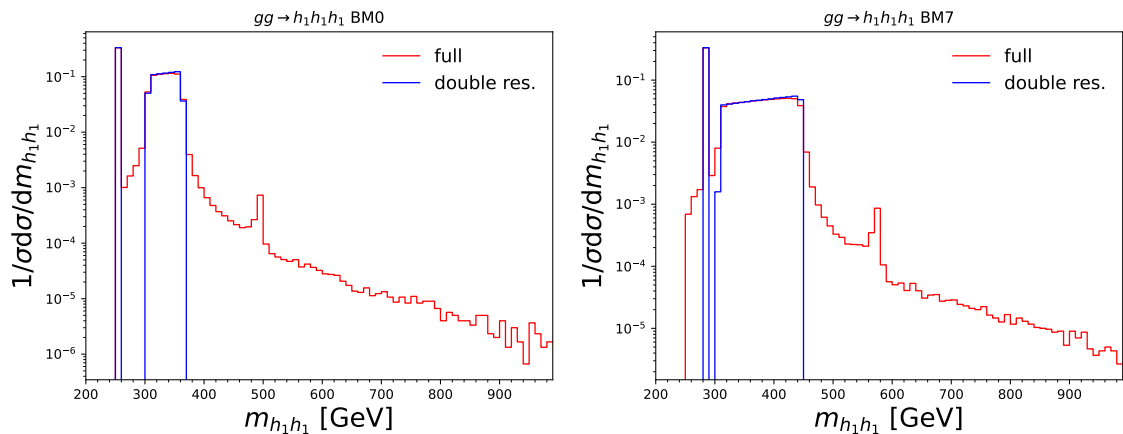


Figure 2: A comparison of the normalized $m_{h_1 h_1}$ distributions, between the full $gg \rightarrow h_1 h_1 h_1$ process and the double-resonant process $gg \rightarrow h_3 \rightarrow h_2 h_1 \rightarrow h_1 h_1 h_1$ for the benchmark points BM0 (left) and BM7 (right) given in Table 1.

any point relevant to any explicit model that contains two heavy scalar particles by rescaling according to eq. 3.4. This is possible since, within the narrow width approximation, event samples generated with the parameters set to unity (i.e. $\rho^2 = 1 \text{ GeV}^2$), will have almost identical kinematics to any other sample after rescaling by ρ^2 . We have performed tests of the extent to which this approximation is reasonable, focusing on the benchmark points derived in ref. [111], which we shown in table 1. Figure 2 shows a normalized comparison of the $m_{h_1 h_1}$ distributions, for the benchmark points BM0 and BM7. One can observe that the “full” process distributions exhibit non-resonant components, represented by the small “continuum” part of the distributions, as well as smaller contributions from $h_3^* \rightarrow h_3 h_1 \rightarrow h_1 h_1 h_1$, where the first h_3 is off shell. Nevertheless, it is clear that an analysis of the double-resonant process will capture the bulk of the total cross section. We present an investigation of the impact of the non-resonant pieces on our phenomenological analysis in sub-section 4.2.

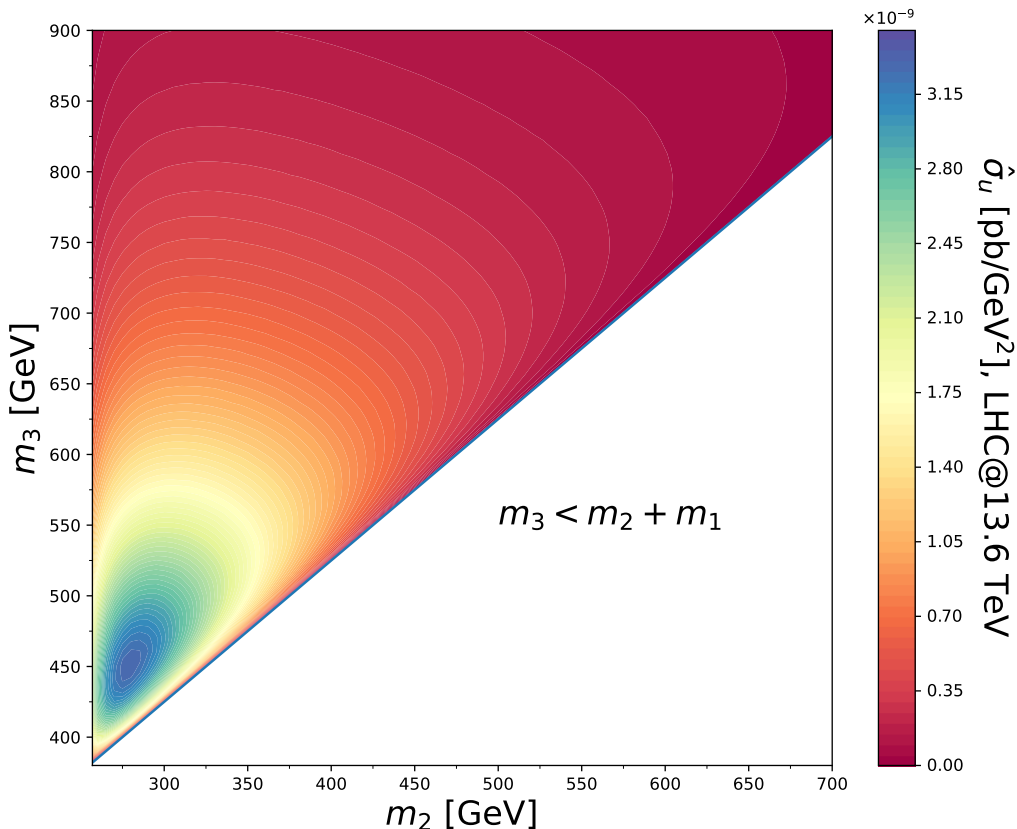


Figure 3: The ‘unity’ cross section $\hat{\sigma}_u$ (eq. 3.4) for the double-resonant triple Higgs boson production process, $gg \rightarrow h_3 \rightarrow h_2 h_1 \rightarrow h_1 h_1 h_1$ at a 13.6 TeV LHC, for $\kappa_3 = 1$, $\lambda_{123} = \lambda_{112} = 1 \text{ GeV}$, and $\Gamma_2 = \Gamma_3 = 1 \text{ GeV}$, interpolated over the (m_2, m_3) -plane.

In practice, one should check the narrow-width requirement on h_3 and h_2 in any explicit model within which the double-resonant process can be generated. Since the scalars are

experimentally constrained to possess small mixing parameters with the SM-like Higgs boson, one way to increase the widths while remaining viable is through scalar-to-scalar decays via scalar triple couplings. In the limit that the scalar decays $h_3 \rightarrow h_2 h_1$ and $h_2 \rightarrow h_1 h_1$ become the dominant ones, ρ^2 tends to a constant value for a given mass combination (m_2, m_3) , since their total widths appear in the denominator of eq. 3.5, and these are proportional to λ_{123}^2 and λ_{112}^2 . This constant value depends on kinematic factors that depend on the scalar masses, and on κ_3^2 , the square of the mixing parameter for the h_3 . For $\kappa_3 \sim \mathcal{O}(1)$, we find that the scalar-dominated value that ρ^2 tends to $\mathcal{O}(10^8 - 10^9 \text{ GeV}^2)$. Therefore, if the limits imposed on ρ^2 are below that value, one would be safely away from the scalar-dominated region, and within the narrow-width scenario. This is the case for the limits that we derive here through our phenomenological analysis.

4 Phenomenological Analysis at the LHC

4.1 Limits on the (m_2, m_3) -plane

To extract limits at the LHC by employing the simplified model defined in section 3, we perform a phenomenological analysis over the (m_2, m_3) -plane, using Monte Carlo signal event samples generated with $\kappa_3 = 1$, $\lambda_{123} = \lambda_{112} = 1 \text{ GeV}$, and $\Gamma_2 = \Gamma_3 = 1 \text{ GeV}$. The parton-level samples were generated using `MadGraph5_aMC@NLO` [116], and the parton shower and non-perturbative effects were simulated through the `HERWIG 7` event generator [117–123]. We consider the dominant QCD-initiated 6b-jet background, $pp \rightarrow 6b$ as well as the sub-dominant $pp \rightarrow Zb\bar{b}b\bar{b}$, $pp \rightarrow ZZb\bar{b}$, $pp \rightarrow h_1 Zb\bar{b}$, $pp \rightarrow h_1 h_1 b\bar{b}$, $pp \rightarrow h_1 h_1 Z$ and $pp \rightarrow h_1 ZZ$, with all the bosons decaying into $b\bar{b}$. As with the case of the signal, we applied a flat k -factor of 2 on all backgrounds. We note here that we have assumed that all backgrounds are SM-like, i.e. we did not consider modifications on the backgrounds due to new physics effects. Since the dominant background by far is the QCD-initiated 6b-jet background, we do not expect this to impact our results. Furthermore, we did not consider any backgrounds originating from misidentification of light or charm jets to b jets, and we did not apply any detector effects beyond the detector acceptance. All jets were reconstructed using the anti- k_T algorithm, with parameter $R = 0.4$ using the `FastJet` library [124]. The b -tagging efficiency was taken to be 85% for true b -jets.

Given that the kinematical distributions are independent of the ρ^2 parameter within the narrow-width approximation, this approach should yield a “once-and-for-all” analysis for double-resonant triple Higgs boson production at the LHC, within *any* model that involves narrow enough scalar resonances, and the masses of two new scalar resonances also satisfy $m_3 > m_2 + m_1$ and $m_2 > 2m_1$. The analysis can be performed point-by-point on the (m_2, m_3) -plane to obtain the optimal signal-versus-background discrimination. Instead, for the sake of clarity and simplicity of presentation, we pursue the definition of a single set of cuts that can be applied everywhere in the interesting region of the (m_2, m_3) -plane. To define the quantity to be maximized over the (m_2, m_3) -plane, consider a pre-selected set of points $i = 1, \dots, N$ that span the plane, e.g. on a grid, while satisfying the necessary mass

hierarchies. Then, we construct the *product* of significances of each point, Σ_{Π} as:

$$\Sigma_{\Pi} \equiv \prod_{i=1}^N \Sigma_i = \prod_{i=1}^N \frac{S_i}{\sqrt{B}}, \quad (4.1)$$

where S_i represent the expected number of signal events for the point i on the (m_2, m_3) -plane, and B the expected number of background events, at an integrated luminosity \mathcal{L} . If the analysis efficiency is ε_i for signal point i , with cross section σ_i before cuts, and $\varepsilon_{B,i}$ is the efficiency for the background, with cross section σ_B before cuts, then we can rewrite Σ_{Π} as:

$$\Sigma_{\Pi} = \left(\prod_{j=1}^N \frac{\sqrt{\mathcal{L}\sigma_j}}{\sqrt{\sigma_B}} \right) \left(\prod_{i=1}^N \frac{\varepsilon_i}{\sqrt{\varepsilon_{B,i}}} \right). \quad (4.2)$$

Therefore, maximizing the second quantity in the product above, which we define as:

$$\mathcal{E}_{\Pi} \equiv \prod_{i=1}^N \frac{\varepsilon_i}{\sqrt{\varepsilon_{B,i}}}, \quad (4.3)$$

will yield the optimal set of cuts over the pre-defined set of points on the (m_2, m_3) -plane. For optimized values, we found that the condition $\frac{\varepsilon_i}{\sqrt{\varepsilon_{B,i}}} > 1$ can easily be satisfied. Therefore, to avoid large numbers in \mathcal{E}_{Π} , we optimize $\log \mathcal{E}_{\Pi}$. We would like to reiterate at this point that this optimization will depend on the set of chosen combinations (m_2, m_3) on the grid, and a full analysis should be performed over the whole plane defined by the masses (m_2, m_3) .

The optimization performed in the present study is based on a subset of 280 combinations for (m_2, m_3) , i.e. 280 signal samples are considered, within the mass windows $260 \leq m_2 \leq 622.3$ GeV and $425 \leq m_3 \leq 1150$ GeV. We select events based on the same procedure followed in ref. [110], and for a detailed description of the observables see section 4.3 therein. Here, we limit ourselves to summarizing the main features of the selection criteria that distinguish the present study from the analysis of ref. [110]. Just as in [110], we select events with at least six b -tagged jets and consider those with the highest transverse momentum. Our optimization focuses on the observables $p_{Tmin,b}$, $\eta_{b,max}$, $\chi^{2,(6)}$, $\chi^{2,(4)}$ and m_{6b}^{inv} . One of the key differences with the procedure followed in [110] is that we find it convenient to explore the parameter space defined by the first four observables in the previous list, by using a random sampling procedure. Thus, we consider random points drawn from the following intervals $p_{Tmin,b} \in [25, 20]$ GeV, $|\eta_{b,max}| \in [0, 3.0]$, $\chi^{2,(6)} \in [5, 60]$ GeV², $\chi^{2,(4)} \in [5, 40]$ GeV². After this first stage, we improve our optimization by imposing a window on m_{6b}^{inv} . We also tested the effect of imposing constraints on m_{4b}^{inv} , but concluded that, in our ‘‘universal’’ cuts approach, this observable does not improve the discrimination power. In particular, when considering the linear rule $m_{4b}^{inv} \leq m_2 + (m_3 - m_2) \times a$, for $0 \leq a \leq 1$, we found that $\log \mathcal{E}_{\Pi}$ is maximized when $a = 1$, rendering a cut on the m_{4b}^{inv} observable irrelevant. As in ref. [110], we consider additional observables, which are however not optimized. The summary of values considered are presented in table 3.

Given the described analysis and the optimized set of cuts, we can derive an expected limit on the ρ^2 parameter over the (m_2, m_3) -plane. To do so, we follow a simple approach

Observable	Constraint
$p_{Tmin,b}$	37.0
$ \eta_{b,max} $	2.95
$\chi^{2,(6)}$	12.0
$\chi^{2,(4)}$	34.0
Δm_{6b}^{inv}	+38.0 -50.0
m_{4b}^{inv}	$\leq m_3$
$p_T(h_1^i)$	$\geq [50, 50, 0]$
$\Delta m_{min,med,max}$	$\geq [15, 14, 20]$
$\Delta R(h_1^i, h_1^j)$	≤ 3.5
$\Delta R_{bb}(h_1)$	≤ 3.5

Table 3: The optimized universal selection cuts used in our phenomenological analysis. Note that the cut on m_{6b}^{inv} should be understood as $m_{6b}^{inv} \in m_3 + \Delta m_{6b}^{inv}$. As in ref. [110], the indices i, j run over the values 1, 2, 3, and refer to the three reconstructed SM-like Higgs bosons. The quantities with units of energy are given in GeV. The observables $\chi^{2,(6)}$ and $\chi^{2,(4)}$ are presented in GeV^2 .

here, first calculating the 95% confidence limit (C.L.) on the cross section, $\sigma_{95\%CL}$, by requiring that the significance,

$$\Sigma = \frac{\varepsilon_S \sigma_S \mathcal{L}}{\sqrt{\varepsilon_B \sigma_B \mathcal{L}}}, \quad (4.4)$$

equals 2 everywhere on the (m_2, m_3) -plane. By setting $\Sigma = 2$, we get $\sigma_S = \sigma_{95\%CL}$:

$$\sigma_{95\%CL} = 2 \frac{\sqrt{\varepsilon_B \sigma_B}}{\varepsilon_S \sqrt{\mathcal{L}}}, \quad (4.5)$$

where σ_B is the total expected background cross section, including the b -tagging efficiencies. The limit on the signal cross section to the particular final state is easily translated into a limit on the total cross section for double-resonant triple Higgs boson production, by taking into account the b -tagging efficiencies and the branching ratios of the Higgs boson into the $b\bar{b}$ final state. All the results are presented here represent limits on the total cross section. This limit is shown in fig. 4, for integrated luminosities of $\mathcal{L} = 300 \text{ fb}^{-1}$ and 3000 fb^{-1} , following our analysis. We note that the order of magnitude of the projected constraint is consistent with the current ATLAS results presented in [114].

We can then proceed to extract the limit on the rescaling parameter, ρ^2 , by dividing out the “unity” cross section (defined by eq. 3.4):

$$\rho_{95\%CL}^2 = \frac{\sigma_{95\%CL}}{\hat{\sigma}_u}, \quad (4.6)$$

where this operation is understood to be taken over the (m_2, m_3) -plane. The results are shown in fig. 5, at a 13.6 TeV LHC, and for integrated luminosities of $\mathcal{L} = 300 \text{ fb}^{-1}$ and 3000 fb^{-1} . To demonstrate the region of the (m_2, m_3) -plane where the double-resonant process can provide information on the TRSM, we have performed a new parameter-space scan that includes the theoretical and experimental constraints as they were imposed in

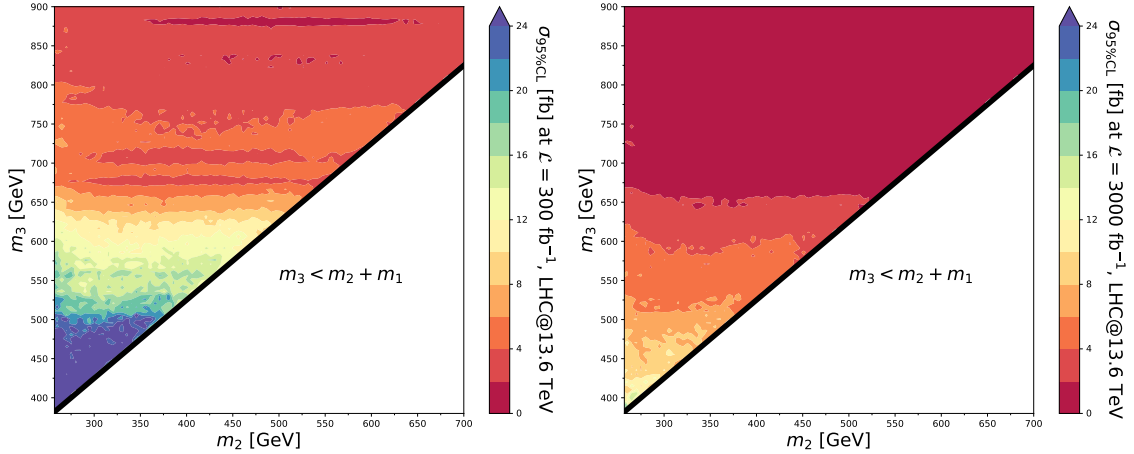


Figure 4: The 95% C.L. on the cross section for double-resonant triple Higgs boson production process, $gg \rightarrow h_3 \rightarrow h_2 h_1 \rightarrow h_1 h_1 h_1$ at a 13.6 TeV LHC, at integrated luminosities of $\mathcal{L} = 300 \text{ fb}^{-1}$ (left) and 3000 fb^{-1} (right).

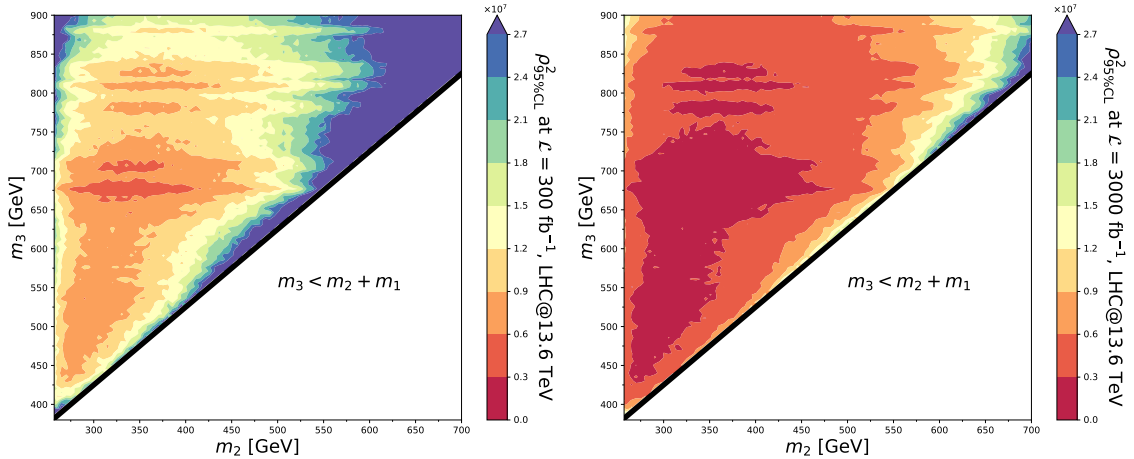


Figure 5: The 95% C.L. limit on the rescaling parameter, ρ^2 for double-resonant triple Higgs boson production process, $gg \rightarrow h_3 \rightarrow h_2 h_1 \rightarrow h_1 h_1 h_1$ at a 13.6 TeV LHC, at integrated luminosities of $\mathcal{L} = 300 \text{ fb}^{-1}$ (left) and 3000 fb^{-1} (right).

ref. [111]. The scan was performed “flat” within the regions of parameters defined by table 4. We note, however, that the density of parameter-space points found here is not meant to be representative of the true statistical distribution of the points in the space of the TRSM, and should not be interpreted as such. A comparison was then made of the ρ^2 value corresponding to each generated point, to the ρ^2 limit at 95% C.L. derived through our analysis. The results are shown in fig. 6 for an integrated luminosity of $\mathcal{L} = 3000 \text{ fb}^{-1}$, where we have also imposed the restrictions that the parameter-space points have a cross section at least 20 times larger than that of SM triple Higgs boson production, and they should

Parameter	Min	Max
m_2	255 GeV	775 GeV
m_3	350 GeV	900 GeV
v_2	0 GeV	1000 GeV
v_3	0 GeV	1000 GeV
k_1	0.95	1.00
k_2	0.00	0.25
k_3	0.00	0.25

Table 4: The range of parameters scanned over, following the theoretical and experimental constraints outlined in ref. [111].

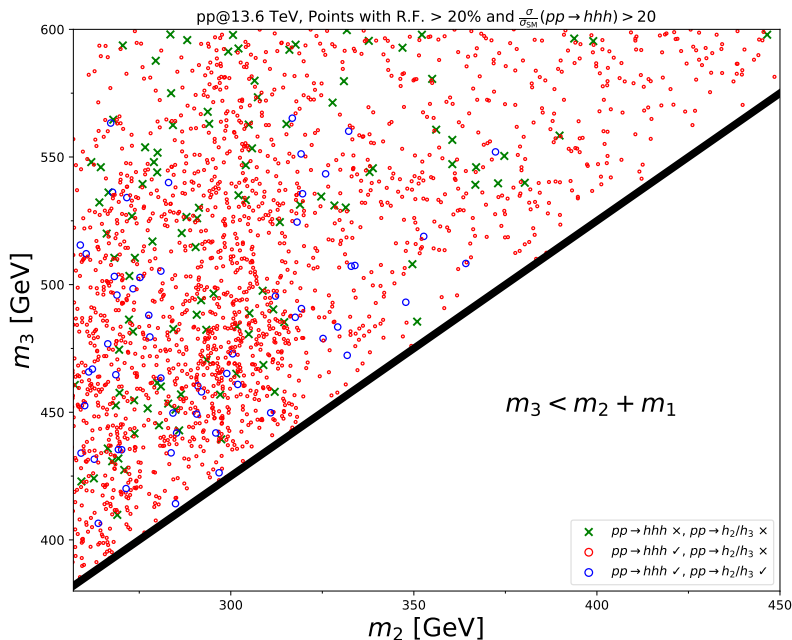


Figure 6: Results for the high-luminosity LHC at 13.6 TeV, with $L = 3000 \text{ fb}^{-1}$. Only points with at least a factor of 20 enhancement over the SM triple Higgs boson production cross section are shown. The points have been selected to satisfy the theoretical and experimental constraints described in ref. [111], and in addition are required to have an approximate double-resonant process contribution to the total cross section of R.F. $\sim 20\%$. We also consider constraints coming from single production of the new scalar resonances $h_{2/3}$, where green crosses indicate points that will be excluded by both double-resonant triple Higgs boson production and single scalar production, red circles indicate points that will be excluded only by single scalar production, and blue circles indicate points that will be excluded by neither.

carry at least 20% of their cross section in the double-resonant process. We also examine the impact of analyses obtained through extrapolations of ATLAS and CMS results, following the procedure outlined in Appendix D of ref. [125]. These originate from the analyses considering the processes $h_i \rightarrow h_1 h_1$ [126, 127], $h_i \rightarrow ZZ$ [128, 129] and $h_i \rightarrow W^+ W^-$ [130, 131], for $i = 2, 3$. A reasonable subset, ~ 100 out of ~ 2000 , of viable parameter-space points can be excluded through double-resonant triple Higgs boson production (green crosses), as well as by single scalar production. We note, however, that a large number of points will remain undetected in this channel, even at the end of the lifetime of the LHC, allowing only an upper limit to be imposed on the ρ^2 parameter, and hence the parameters by which it is constructed. Nevertheless, a large fraction of the parameter-space points will likely be excluded through single h_2 or h_3 production (red circles), with a smaller number evading these searches as well (blue circles). We anticipate that for the parameter-space points that evade all searches, a collider such as the FCC-hh with a proton-proton center-of-mass energy of 100 TeV will be necessary, see e.g. [125]. Finally, we also note that we have found *no* points that will remain undetected in single scalar production, and at the same time detected in double-resonant triple Higgs boson production. This is suggestive to the fact that triple Higgs boson production will unlikely play the role of a discovery channel for the two new scalar resonances in the TRSM.

It is also interesting to note that during our parameter-space scan for experimentally- and theoretically-viable points within the TRSM, we did not obtain any with $m_3 \gtrsim 650$ GeV or $m_2 \gtrsim 450$ GeV that also satisfy the $\times 20$ enhancement over the SM triple Higgs boson production. This hints towards a rapid decrease of the resonant triple Higgs boson cross section in those regions of parameter space. We would like to point out an similar finding in ref. [132], where the complex singlet model was investigated, see appendix C of the aforementioned reference.

4.2 Case Studies: Resonant Versus Full Non-Resonant Production at the LHC

It is interesting to investigate the impact on our analysis of the inevitable non-resonant components of the triple Higgs boson production process. Since the SM triple Higgs boson production cross section is tiny, and interference effects are expected to be small, we do not expect a priori to have a significant impact on our results. To estimate this effect, for the points that have achieved a 95% C.L. exclusion at the high-luminosity LHC through our analysis (green crosses in fig. 6), we have considered both the full leading-order triple Higgs boson production process, including the non-resonant components, and double-resonant triple Higgs boson production Monte Carlo event samples. We applied our phenomenological analysis on both samples.

A sample of the six b -jet invariant mass after all other cuts have been applied, comparing the two distributions obtained from the full process and the double-resonant process only is shown in fig. 7, for six parameter-space points that can be excluded at the high-luminosity LHC. We have also estimated the expected significance for both cases after all cuts, and the fractional change between them. A frequency plot of the expected change in statistical significance is shown in fig. 8 for the $\mathcal{O}(100)$ parameter-space points, demonstrating that the change is expected to be marginal, with most parameter-space points possessing a

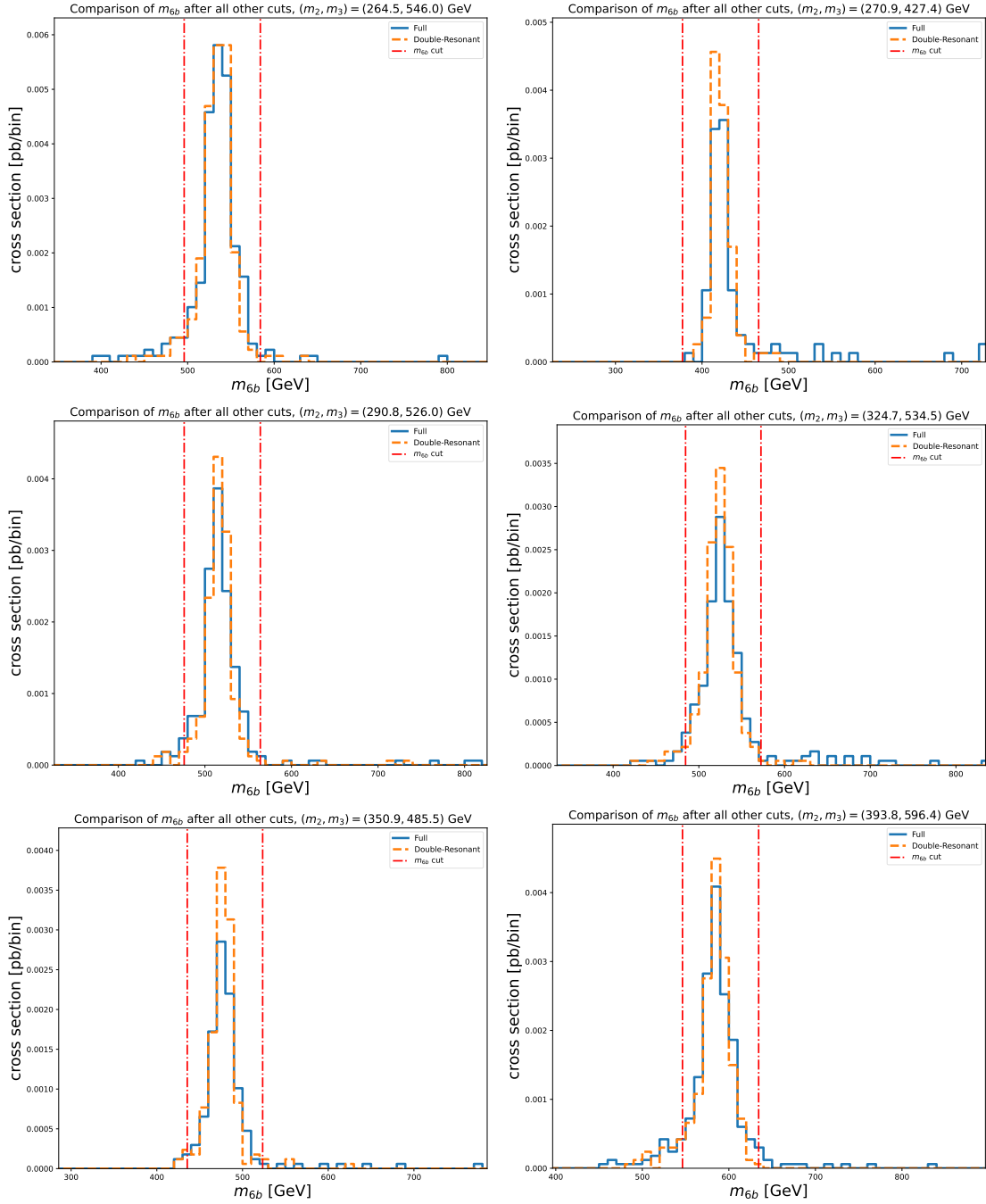


Figure 7: A comparison of the six b -jet invariant mass distributions, m_{6b} , obtained through the analysis of the full and double-resonant. All other cuts have been applied, apart from the m_{6b} window, shown in the red dashed-dotted lines.

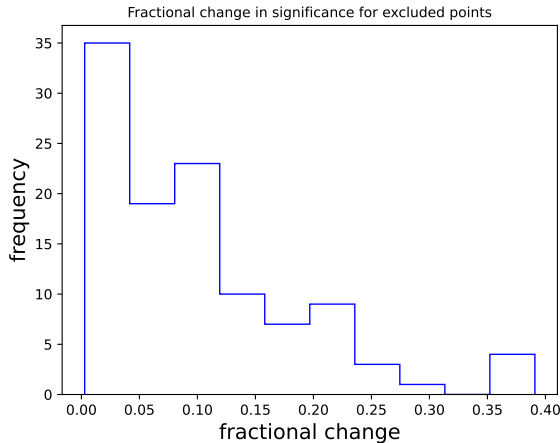


Figure 8: Frequency histogram of the fractional change in the statistical significance of our analysis between Monte Carlo event samples for the full triple Higgs boson production process and the double-resonant process. The analysis was performed at the high-luminosity LHC with an integrated luminosity of 3000 fb^{-1} , for those points that our analysis is expected to exclude at 95% C.L..

$\mathcal{O}(10\%)$ change in the number of standard deviations. We emphasize the fact that since no smearing was applied to simulate detector effects, beyond those appearing due to the Monte Carlo simulation of hadronization, we expect any actual experimental results to exhibit even smaller differences in a more realistic analysis.

5 Conclusions

We have developed a simplified approach to investigating double-resonant triple Higgs boson production, $pp \rightarrow h_3 \rightarrow h_2 h_1 \rightarrow h_1 h_1 h_1$, in models with extended scalar sectors that include at least two new, narrow, scalar resonances that mix with the SM-like Higgs boson. The process is characterized by a single rescaling parameter, which we dub ρ^2 , that constitutes a function of all relevant parameters that determine the cross section for the process. The kinematic distributions in this simplified approach are otherwise independent of the scalar couplings λ_{112} , λ_{123} , the mixing parameter κ_3 , and the widths of the new scalars, as long as the latter are small enough compared to the scalar masses (i.e. $\Gamma_{2,3} \ll m_{2,3}$). We have used this approach to study the parameter space of the TRSM, a model with two new singlet scalar fields S and X , with discrete symmetries \mathbb{Z}_2^S and \mathbb{Z}_2^X . We find, empirically, that significantly-enhanced triple Higgs boson production is limited to the range of masses $m_3 \lesssim 650 \text{ GeV}$ or $m_2 \lesssim 450 \text{ GeV}$, and that it can be excluded for a subset of these points, while single heavy scalar production will exclude the majority of the investigated points. We also found that some of these points will remain viable, even at the end of the high-luminosity LHC, and that triple Higgs boson production will unlikely play the role of a discovery channel for the TRSM. Finally, we investigated the contribution of the non-resonant part of the process to our analysis, finding that, at least at the LHC, the non-

resonant part will not contribute meaningfully to the signal. Our approach can be applied to any model with two new narrow scalar resonances that is able to generate the double-resonant decay chain, and will allow the interpretation of experimental results in terms of the theoretical parameter space of models with extended scalar sectors, contributing towards the solution of the inverse problem in the case of discovery.

Acknowledgments

We would like to thank Tania Robens for useful comments and discussions during the mini-workshop on “HHH and other extended scalar sector signatures” at the Ruđer Bošković Institute, Zagreb, Croatia, in July 2024. We would also like to thank Ian Lewis for useful discussions during the “Extended Scalar Sectors From All Angles” workshop at CERN, in October 2024. A.P. acknowledges support by the National Science Foundation under Grant No. PHY 2210161. G.T.X. received support for this project from the European Union’s Horizon 2020 research and innovation programme under the Marie Skłodowska-Curie grant agreement No 945422. This research was supported by the Deutsche Forschungsgemeinschaft (DFG, German Research Foundation) under grant 396021762 - TRR 257.

References

- [1] ATLAS collaboration, *Observation of a new particle in the search for the Standard Model Higgs boson with the ATLAS detector at the LHC*, *Phys. Lett. B* **716** (2012) 1 [[1207.7214](#)].
- [2] CMS collaboration, *Observation of a New Boson at a Mass of 125 GeV with the CMS Experiment at the LHC*, *Phys. Lett. B* **716** (2012) 30 [[1207.7235](#)].
- [3] P.W. Higgs, *Broken Symmetries and the Masses of Gauge Bosons*, *Phys. Rev. Lett.* **13** (1964) 508.
- [4] F. Englert and R. Brout, *Broken Symmetry and the Mass of Gauge Vector Mesons*, *Phys. Rev. Lett.* **13** (1964) 321.
- [5] G.S. Guralnik, C.R. Hagen and T.W.B. Kibble, *Global Conservation Laws and Massless Particles*, *Phys. Rev. Lett.* **13** (1964) 585.
- [6] CMS collaboration, *Search for Higgs boson pair production in the $b\bar{b}\tau\tau$ final state in proton-proton collisions at $\sqrt{s} = 8$ TeV*, *Phys. Rev. D* **96** (2017) 072004 [[1707.00350](#)].
- [7] CMS collaboration, *Search for Higgs boson pair production in events with two bottom quarks and two tau leptons in proton-proton collisions at $\sqrt{s} = 13$ TeV*, *Phys. Lett. B* **778** (2018) 101 [[1707.02909](#)].
- [8] CMS collaboration, *Search for resonant and nonresonant Higgs boson pair production in the $b\bar{b}l\nu l\nu$ final state in proton-proton collisions at $\sqrt{s} = 13$ TeV*, *JHEP* **01** (2018) 054 [[1708.04188](#)].
- [9] CMS collaboration, *Search for Higgs boson pair production in the $\gamma\gamma b\bar{b}$ final state in pp collisions at $\sqrt{s} = 13$ TeV*, *Phys. Lett. B* **788** (2019) 7 [[1806.00408](#)].
- [10] CMS collaboration, *Search for production of Higgs boson pairs in the four b quark final state using large-area jets in proton-proton collisions at $\sqrt{s} = 13$ TeV*, *JHEP* **01** (2019) 040 [[1808.01473](#)].

- [11] CMS collaboration, *Search for nonresonant Higgs boson pair production in the $b\bar{b}b\bar{b}$ final state at $\sqrt{s} = 13$ TeV*, *JHEP* **04** (2019) 112 [[1810.11854](#)].
- [12] CMS collaboration, *Combination of searches for Higgs boson pair production in proton-proton collisions at $\sqrt{s} = 13$ TeV*, *Phys. Rev. Lett.* **122** (2019) 121803 [[1811.09689](#)].
- [13] CMS collaboration, *Search for nonresonant Higgs boson pair production in final states with two bottom quarks and two photons in proton-proton collisions at $\sqrt{s} = 13$ TeV*, *JHEP* **03** (2021) 257 [[2011.12373](#)].
- [14] CMS collaboration, *Search for Higgs Boson Pair Production in the Four b Quark Final State in Proton-Proton Collisions at $s=13$ TeV*, *Phys. Rev. Lett.* **129** (2022) 081802 [[2202.09617](#)].
- [15] CMS collaboration, *Search for nonresonant Higgs boson pair production in final state with two bottom quarks and two tau leptons in proton-proton collisions at $s=13$ TeV*, *Phys. Lett. B* **842** (2023) 137531 [[2206.09401](#)].
- [16] CMS collaboration, *Search for Higgs boson pairs decaying to WW^*WW^* , $WW^*\tau\tau$, and $\tau\tau\tau\tau$ in proton-proton collisions at $\sqrt{s} = 13$ TeV*, *JHEP* **07** (2023) 095 [[2206.10268](#)].
- [17] CMS collaboration, *Search for nonresonant Higgs boson pair production in the four leptons plus two jets final state in proton-proton collisions at $\sqrt{s} = 13$ TeV*, *JHEP* **06** (2023) 130 [[2206.10657](#)].
- [18] ATLAS collaboration, *Search For Higgs Boson Pair Production in the $\gamma\gamma b\bar{b}$ Final State using pp Collision Data at $\sqrt{s} = 8$ TeV from the ATLAS Detector*, *Phys. Rev. Lett.* **114** (2015) 081802 [[1406.5053](#)].
- [19] ATLAS collaboration, *Search for Higgs boson pair production in the $b\bar{b}b\bar{b}$ final state from pp collisions at $\sqrt{s} = 8$ TeV with the ATLAS detector*, *Eur. Phys. J. C* **75** (2015) 412 [[1506.00285](#)].
- [20] ATLAS collaboration, *Searches for Higgs boson pair production in the $hh \rightarrow b\bar{b}\tau\tau, \gamma\gamma WW^*, \gamma\gamma b\bar{b}, b\bar{b}b\bar{b}$ channels with the ATLAS detector*, *Phys. Rev. D* **92** (2015) 092004 [[1509.04670](#)].
- [21] ATLAS collaboration, *Search for pair production of Higgs bosons in the $b\bar{b}b\bar{b}$ final state using proton-proton collisions at $\sqrt{s} = 13$ TeV with the ATLAS detector*, *Phys. Rev. D* **94** (2016) 052002 [[1606.04782](#)].
- [22] ATLAS collaboration, *Search for pair production of Higgs bosons in the $b\bar{b}b\bar{b}$ final state using proton-proton collisions at $\sqrt{s} = 13$ TeV with the ATLAS detector*, *JHEP* **01** (2019) 030 [[1804.06174](#)].
- [23] ATLAS collaboration, *Search for Higgs boson pair production in the $\gamma\gamma b\bar{b}$ final state with 13 TeV pp collision data collected by the ATLAS experiment*, *JHEP* **11** (2018) 040 [[1807.04873](#)].
- [24] ATLAS collaboration, *Search for Higgs boson pair production in the $\gamma\gamma WW^*$ channel using pp collision data recorded at $\sqrt{s} = 13$ TeV with the ATLAS detector*, *Eur. Phys. J. C* **78** (2018) 1007 [[1807.08567](#)].
- [25] ATLAS collaboration, *Search for resonant and non-resonant Higgs boson pair production in the $b\bar{b}\tau^+\tau^-$ decay channel in pp collisions at $\sqrt{s} = 13$ TeV with the ATLAS detector*, *Phys. Rev. Lett.* **121** (2018) 191801 [[1808.00336](#)].

- [26] ATLAS collaboration, *Search for Higgs boson pair production in the $b\bar{b}W^*W^*$ decay mode at $\sqrt{s} = 13$ TeV with the ATLAS detector*, *JHEP* **04** (2019) 092 [[1811.04671](#)].
- [27] ATLAS collaboration, *Search for Higgs boson pair production in the $WW^{(*)}WW^{(*)}$ decay channel using ATLAS data recorded at $\sqrt{s} = 13$ TeV*, *JHEP* **05** (2019) 124 [[1811.11028](#)].
- [28] ATLAS collaboration, *Combination of searches for Higgs boson pairs in pp collisions at $\sqrt{s} = 13$ TeV with the ATLAS detector*, *Phys. Lett. B* **800** (2020) 135103 [[1906.02025](#)].
- [29] ATLAS collaboration, *Search for non-resonant Higgs boson pair production in the $b\bar{b}\nu\bar{\nu}$ final state with the ATLAS detector in pp collisions at $\sqrt{s} = 13$ TeV*, *Phys. Lett. B* **801** (2020) 135145 [[1908.06765](#)].
- [30] ATLAS collaboration, *Search for the $HH \rightarrow b\bar{b}b\bar{b}$ process via vector-boson fusion production using proton-proton collisions at $\sqrt{s} = 13$ TeV with the ATLAS detector*, *JHEP* **07** (2020) 108 [[2001.05178](#)].
- [31] ATLAS collaboration, *Search for Higgs boson pair production in the two bottom quarks plus two photons final state in pp collisions at $\sqrt{s} = 13$ TeV with the ATLAS detector*, *Phys. Rev. D* **106** (2022) 052001 [[2112.11876](#)].
- [32] ATLAS collaboration, *Search for resonant and non-resonant Higgs boson pair production in the $b\bar{b}\tau^+\tau^-$ decay channel using 13 TeV pp collision data from the ATLAS detector*, *JHEP* **07** (2023) 040 [[2209.10910](#)].
- [33] ATLAS collaboration, *Constraints on the Higgs boson self-coupling from single- and double-Higgs production with the ATLAS detector using pp collisions at $s=13$ TeV*, *Phys. Lett. B* **843** (2023) 137745 [[2211.01216](#)].
- [34] ATLAS collaboration, *Search for nonresonant pair production of Higgs bosons in the $b\bar{b}b\bar{b}$ final state in pp collisions at $s=13$ TeV with the ATLAS detector*, *Phys. Rev. D* **108** (2023) 052003 [[2301.03212](#)].
- [35] ATLAS collaboration, *Studies of new Higgs boson interactions through nonresonant HH production in the $b\bar{b}\gamma\gamma$ final state in pp collisions at $\sqrt{s} = 13$ TeV with the ATLAS detector*, [2310.12301](#).
- [36] U. Baur, T. Plehn and D.L. Rainwater, *Measuring the Higgs Boson Self Coupling at the LHC and Finite Top Mass Matrix Elements*, *Phys. Rev. Lett.* **89** (2002) 151801 [[hep-ph/0206024](#)].
- [37] U. Baur, T. Plehn and D.L. Rainwater, *Determining the Higgs Boson Selfcoupling at Hadron Colliders*, *Phys. Rev. D* **67** (2003) 033003 [[hep-ph/0211224](#)].
- [38] U. Baur, T. Plehn and D.L. Rainwater, *Probing the Higgs selfcoupling at hadron colliders using rare decays*, *Phys. Rev. D* **69** (2004) 053004 [[hep-ph/0310056](#)].
- [39] M.J. Dolan, C. Englert and M. Spannowsky, *New Physics in LHC Higgs boson pair production*, *Phys. Rev. D* **87** (2013) 055002 [[1210.8166](#)].
- [40] A. Papaefstathiou, L.L. Yang and J. Zurita, *Higgs boson pair production at the LHC in the $b\bar{b}W^+W^-$ channel*, *Phys. Rev. D* **87** (2013) 011301 [[1209.1489](#)].
- [41] J. Cao, Z. Heng, L. Shang, P. Wan and J.M. Yang, *Pair Production of a 125 GeV Higgs Boson in MSSM and NMSSM at the LHC*, *JHEP* **04** (2013) 134 [[1301.6437](#)].
- [42] F. Goertz, A. Papaefstathiou, L.L. Yang and J. Zurita, *Higgs Boson self-coupling measurements using ratios of cross sections*, *JHEP* **06** (2013) 016 [[1301.3492](#)].

- [43] A. Arbey, M. Battaglia and F. Mahmoudi, *Supersymmetric Heavy Higgs Bosons at the LHC*, *Phys. Rev. D* **88** (2013) 015007 [[1303.7450](#)].
- [44] D. de Florian and J. Mazzitelli, *Two-loop virtual corrections to Higgs pair production*, *Phys. Lett. B* **724** (2013) 306 [[1305.5206](#)].
- [45] R.S. Gupta, H. Rzehak and J.D. Wells, *How well do we need to measure the Higgs boson mass and self-coupling?*, *Phys. Rev. D* **88** (2013) 055024 [[1305.6397](#)].
- [46] U. Ellwanger, *Higgs pair production in the NMSSM at the LHC*, *JHEP* **08** (2013) 077 [[1306.5541](#)].
- [47] A.J. Barr, M.J. Dolan, C. Englert and M. Spannowsky, *Di-Higgs final states augMT2ed – selecting hh events at the high luminosity LHC*, *Phys. Lett. B* **728** (2014) 308 [[1309.6318](#)].
- [48] P. Maierhöfer and A. Papaefstathiou, *Higgs Boson pair production merged to one jet*, *JHEP* **03** (2014) 126 [[1401.0007](#)].
- [49] D. de Florian and J. Mazzitelli, *Higgs Boson Pair Production at Next-to-Next-to-Leading Order in QCD*, *Phys. Rev. Lett.* **111** (2013) 201801 [[1309.6594](#)].
- [50] M.J. Dolan, C. Englert, N. Greiner and M. Spannowsky, *Further on up the road: hhjj production at the LHC*, *Phys. Rev. Lett.* **112** (2014) 101802 [[1310.1084](#)].
- [51] F. Goertz, A. Papaefstathiou, L.L. Yang and J. Zurita, *Measuring the Higgs boson self-coupling at the LHC using ratios of cross sections*, in *25th Rencontres de Blois on Particle Physics and Cosmology*, 9, 2013 [[1309.3805](#)].
- [52] F. Goertz, A. Papaefstathiou, L.L. Yang and J. Zurita, *Higgs boson pair production in the D=6 extension of the SM*, *JHEP* **04** (2015) 167 [[1410.3471](#)].
- [53] A. Azatov, R. Contino, G. Panico and M. Son, *Effective field theory analysis of double Higgs boson production via gluon fusion*, *Phys. Rev. D* **92** (2015) 035001 [[1502.00539](#)].
- [54] R. Frederix, S. Frixione, V. Hirschi, F. Maltoni, O. Mattelaer, P. Torrielli et al., *Higgs pair production at the LHC with NLO and parton-shower effects*, *Phys. Lett. B* **732** (2014) 142 [[1401.7340](#)].
- [55] J. Baglio, O. Eberhardt, U. Nierste and M. Wiebusch, *Benchmarks for Higgs Pair Production and Heavy Higgs boson Searches in the Two-Higgs-Doublet Model of Type II*, *Phys. Rev. D* **90** (2014) 015008 [[1403.1264](#)].
- [56] D.E. Ferreira de Lima, A. Papaefstathiou and M. Spannowsky, *Standard model Higgs boson pair production in the $(b\bar{b})(b\bar{b})$ final state*, *JHEP* **08** (2014) 030 [[1404.7139](#)].
- [57] D. de Florian and J. Mazzitelli, *Next-to-Next-to-Leading Order QCD Corrections to Higgs Boson Pair Production*, *PoS* **LL2014** (2014) 029 [[1405.4704](#)].
- [58] B. Hespel, D. Lopez-Val and E. Vryonidou, *Higgs pair production via gluon fusion in the Two-Higgs-Doublet Model*, *JHEP* **09** (2014) 124 [[1407.0281](#)].
- [59] V. Barger, L.L. Everett, C.B. Jackson, A.D. Peterson and G. Shaughnessy, *New physics in resonant production of Higgs boson pairs*, *Phys. Rev. Lett.* **114** (2015) 011801 [[1408.0003](#)].
- [60] S.I. Godunov, M.I. Vysotsky and E.V. Zhemchugov, *Double Higgs production at LHC, see-saw type II and Georgi-Machacek model*, *J. Exp. Theor. Phys.* **120** (2015) 369 [[1408.0184](#)].
- [61] N. Liu, S. Hu, B. Yang and J. Han, *Impact of top-Higgs couplings on Di-Higgs production at future colliders*, *JHEP* **01** (2015) 008 [[1408.4191](#)].

- [62] F. Maltoni, E. Vryonidou and M. Zaro, *Top-quark mass effects in double and triple Higgs production in gluon-gluon fusion at NLO*, *JHEP* **11** (2014) 079 [[1408.6542](#)].
- [63] C.-Y. Chen, S. Dawson and I.M. Lewis, *Exploring resonant di-Higgs boson production in the Higgs singlet model*, *Phys. Rev. D* **91** (2015) 035015 [[1410.5488](#)].
- [64] A.J. Barr, M.J. Dolan, C. Englert, D.E. Ferreira de Lima and M. Spannowsky, *Higgs Self-Coupling Measurements at a 100 TeV Hadron Collider*, *JHEP* **02** (2015) 016 [[1412.7154](#)].
- [65] V. Martín Lozano, J.M. Moreno and C.B. Park, *Resonant Higgs boson pair production in the $hh \rightarrow b\bar{b} WW \rightarrow b\bar{b}\ell^+\nu\ell^-\bar{\nu}$ decay channel*, *JHEP* **08** (2015) 004 [[1501.03799](#)].
- [66] A. Papaefstathiou, *Discovering Higgs boson pair production through rare final states at a 100 TeV collider*, *Phys. Rev. D* **91** (2015) 113016 [[1504.04621](#)].
- [67] S. Dawson, A. Ismail and I. Low, *What's in the loop? The anatomy of double Higgs production*, *Phys. Rev. D* **91** (2015) 115008 [[1504.05596](#)].
- [68] A.V. Kotwal, S. Chekanov and M. Low, *Double Higgs Boson Production in the 4τ Channel from Resonances in Longitudinal Vector Boson Scattering at a 100 TeV Collider*, *Phys. Rev. D* **91** (2015) 114018 [[1504.08042](#)].
- [69] C.-T. Lu, J. Chang, K. Cheung and J.S. Lee, *An exploratory study of Higgs-boson pair production*, *JHEP* **08** (2015) 133 [[1505.00957](#)].
- [70] A. Carvalho, M. Dall'Osso, T. Dorigo, F. Goertz, C.A. Gottardo and M. Tosi, *Higgs Pair Production: Choosing Benchmarks With Cluster Analysis*, *JHEP* **04** (2016) 126 [[1507.02245](#)].
- [71] Q.-H. Cao, Y. Liu and B. Yan, *Measuring trilinear Higgs coupling in WHH and ZHH productions at the high-luminosity LHC*, *Phys. Rev. D* **95** (2017) 073006 [[1511.03311](#)].
- [72] B. Batell, M. McCullough, D. Stolarski and C.B. Verhaaren, *Putting a Stop to di-Higgs Modifications*, *JHEP* **09** (2015) 216 [[1508.01208](#)].
- [73] S. Dawson and I.M. Lewis, *NLO corrections to double Higgs boson production in the Higgs singlet model*, *Phys. Rev. D* **92** (2015) 094023 [[1508.05397](#)].
- [74] Q.-H. Cao, B. Yan, D.-M. Zhang and H. Zhang, *Resolving the Degeneracy in Single Higgs Production with Higgs Pair Production*, *Phys. Lett. B* **752** (2016) 285 [[1508.06512](#)].
- [75] S. Kanemura, K. Kaneta, N. Machida, S. Odori and T. Shindou, *Single and double production of the Higgs boson at hadron and lepton colliders in minimal composite Higgs models*, *Phys. Rev. D* **94** (2016) 015028 [[1603.05588](#)].
- [76] R. Contino et al., *Physics at a 100 TeV pp collider: Higgs and EW symmetry breaking studies*, [1606.09408](#).
- [77] Q.-H. Cao, G. Li, B. Yan, D.-M. Zhang and H. Zhang, *Double Higgs production at the 14 TeV LHC and a 100 TeV pp collider*, *Phys. Rev. D* **96** (2017) 095031 [[1611.09336](#)].
- [78] S. Banerjee, B. Batell and M. Spannowsky, *Invisible decays in Higgs boson pair production*, *Phys. Rev. D* **95** (2017) 035009 [[1608.08601](#)].
- [79] T. Huang, J.M. No, L. Pernié, M. Ramsey-Musolf, A. Safonov, M. Spannowsky et al., *Resonant di-Higgs boson production in the $b\bar{b}WW$ channel: Probing the electroweak phase transition at the LHC*, *Phys. Rev. D* **96** (2017) 035007 [[1701.04442](#)].

- [80] K. Nakamura, K. Nishiwaki, K.-y. Oda, S.C. Park and Y. Yamamoto, *Di-higgs enhancement by neutral scalar as probe of new colored sector*, *Eur. Phys. J. C* **77** (2017) 273 [[1701.06137](#)].
- [81] I.M. Lewis and M. Sullivan, *Benchmarks for Double Higgs Production in the Singlet Extended Standard Model at the LHC*, *Phys. Rev. D* **96** (2017) 035037 [[1701.08774](#)].
- [82] L. Di Luzio, R. Gröber and M. Spannowsky, *Maxi-sizing the trilinear Higgs self-coupling: how large could it be?*, *Eur. Phys. J. C* **77** (2017) 788 [[1704.02311](#)].
- [83] R. Grober, M. Muhlleitner and M. Spira, *Higgs Pair Production at NLO QCD for CP-violating Higgs Sectors*, *Nucl. Phys. B* **925** (2017) 1 [[1705.05314](#)].
- [84] J. Zurita, *Di-Higgs production at the LHC and beyond*, in *5th Large Hadron Collider Physics Conference*, 8, 2017 [[1708.00892](#)].
- [85] E. Arganda, J.L. Díaz-Cruz, N. Mileo, R.A. Morales and A. Szyrkman, *Search strategies for pair production of heavy Higgs bosons decaying invisibly at the LHC*, *Nucl. Phys. B* **929** (2018) 171 [[1710.07254](#)].
- [86] A. Adhikary, S. Banerjee, R.K. Barman, B. Bhattacharjee and S. Niyogi, *Revisiting the non-resonant Higgs pair production at the HL-LHC*, *JHEP* **07** (2018) 116 [[1712.05346](#)].
- [87] M. Bauer, M. Carena and A. Carmona, *Higgs Pair Production as a Signal of Enhanced Yukawa Couplings*, *Phys. Rev. Lett.* **121** (2018) 021801 [[1801.00363](#)].
- [88] F. Maltoni, D. Pagani and X. Zhao, *Constraining the Higgs self-couplings at $e+e-$ colliders*, *JHEP* **07** (2018) 087 [[1802.07616](#)].
- [89] S. Borowka, C. Duhr, F. Maltoni, D. Pagani, A. Shivaji and X. Zhao, *Probing the scalar potential via double Higgs boson production at hadron colliders*, *JHEP* **04** (2019) 016 [[1811.12366](#)].
- [90] D. Gonçalves, T. Han, F. Kling, T. Plehn and M. Takeuchi, *Higgs boson pair production at future hadron colliders: From kinematics to dynamics*, *Phys. Rev. D* **97** (2018) 113004 [[1802.04319](#)].
- [91] J. Chang, K. Cheung, J.S. Lee, C.-T. Lu and J. Park, *Higgs-boson-pair production $H(\rightarrow bb^-)H(\rightarrow \gamma\gamma)$ from gluon fusion at the HL-LHC and HL-100 TeV hadron collider*, *Phys. Rev. D* **100** (2019) 096001 [[1804.07130](#)].
- [92] P. Basler, S. Dawson, C. Englert and M. Mühlleitner, *Showcasing HH production: Benchmarks for the LHC and HL-LHC*, *Phys. Rev. D* **99** (2019) 055048 [[1812.03542](#)].
- [93] A. Adhikary, S. Banerjee, R. Kumar Barman and B. Bhattacharjee, *Resonant heavy Higgs searches at the HL-LHC*, *JHEP* **09** (2019) 068 [[1812.05640](#)].
- [94] J. Alison et al., *Higgs boson potential at colliders: Status and perspectives*, *Rev. Phys.* **5** (2020) 100045 [[1910.00012](#)].
- [95] G. Li, L.-X. Xu, B. Yan and C.P. Yuan, *Resolving the degeneracy in top quark Yukawa coupling with Higgs pair production*, *Phys. Lett. B* **800** (2020) 135070 [[1904.12006](#)].
- [96] K. Cheung, A. Jueid, C.-T. Lu, J. Song and Y.W. Yoon, *Disentangling new physics effects on nonresonant Higgs boson pair production from gluon fusion*, *Phys. Rev. D* **103** (2021) 015019 [[2003.11043](#)].
- [97] P.N. Bhattiprolu and J.D. Wells, *Sensitivity target for an impactful Higgs boson self coupling measurement*, [2407.11847](#).

- [98] T. Plehn and M. Rauch, *The quartic higgs coupling at hadron colliders*, *Phys. Rev. D* **72** (2005) 053008 [[hep-ph/0507321](#)].
- [99] A. Papaefstathiou and K. Sakurai, *Triple Higgs boson production at a 100 TeV proton-proton collider*, *JHEP* **02** (2016) 006 [[1508.06524](#)].
- [100] C.-Y. Chen, Q.-S. Yan, X. Zhao, Y.-M. Zhong and Z. Zhao, *Probing triple-Higgs productions via $4b2\gamma$ decay channel at a 100 TeV hadron collider*, *Phys. Rev. D* **93** (2016) 013007 [[1510.04013](#)].
- [101] B. Fuks, J.H. Kim and S.J. Lee, *Probing Higgs self-interactions in proton-proton collisions at a center-of-mass energy of 100 TeV*, *Phys. Rev. D* **93** (2016) 035026 [[1510.07697](#)].
- [102] A. Papaefstathiou, *Multi-Higgs Boson Production and Self-coupling Measurements at Hadron Colliders*, *Acta Phys. Polon. B* **48** (2017) 1133.
- [103] B. Fuks, J.H. Kim and S.J. Lee, *Scrutinizing the Higgs quartic coupling at a future 100 TeV proton-proton collider with taus and b-jets*, *Phys. Lett. B* **771** (2017) 354 [[1704.04298](#)].
- [104] T. Liu, K.-F. Lyu, J. Ren and H.X. Zhu, *Probing the quartic Higgs boson self-interaction*, *Phys. Rev. D* **98** (2018) 093004 [[1803.04359](#)].
- [105] A. Papaefstathiou, G. Tetlalmatzi-Xolocotzi and M. Zaro, *Triple Higgs boson production to six b-jets at a 100 TeV proton collider*, *Eur. Phys. J. C* **79** (2019) 947 [[1909.09166](#)].
- [106] D. de Florian, I. Fabre and J. Mazzitelli, *Triple Higgs production at hadron colliders at NNLO in QCD*, *JHEP* **03** (2020) 155 [[1912.02760](#)].
- [107] M. Chiesa, F. Maltoni, L. Mantani, B. Mele, F. Piccinini and X. Zhao, *Measuring the quartic Higgs self-coupling at a multi-TeV muon collider*, *JHEP* **09** (2020) 098 [[2003.13628](#)].
- [108] M. Abdughani, D. Wang, L. Wu, J.M. Yang and J. Zhao, *Probing the triple Higgs boson coupling with machine learning at the LHC*, *Phys. Rev. D* **104** (2021) 056003 [[2005.11086](#)].
- [109] T. Robens, T. Stefaniak and J. Wittbrodt, *Two-real-scalar-singlet extension of the SM: LHC phenomenology and benchmark scenarios*, *Eur. Phys. J. C* **80** (2020) 151 [[1908.08554](#)].
- [110] A. Papaefstathiou, T. Robens and G. Tetlalmatzi-Xolocotzi, *Triple Higgs Boson Production at the Large Hadron Collider with Two Real Singlet Scalars*, *JHEP* **05** (2021) 193 [[2101.00037](#)].
- [111] O. Karkout, A. Papaefstathiou, M. Postma, G. Tetlalmatzi-Xolocotzi, J. van de Vis and T. du Pree, *Triple Higgs boson production and electroweak phase transition in the two-real-singlet model*, [2404.12425](#).
- [112] P. Stylianou and G. Weiglein, *Constraints on the trilinear and quartic Higgs couplings from triple Higgs production at the LHC and beyond*, *Eur. Phys. J. C* **84** (2024) 366 [[2312.04646](#)].
- [113] A. Papaefstathiou and G. Tetlalmatzi-Xolocotzi, *Multi-Higgs boson production with anomalous interactions at current and future proton colliders*, *JHEP* **06** (2024) 124 [[2312.13562](#)].
- [114] ATLAS collaboration, *A search for triple Higgs boson production in the $6b$ final state using pp collisions at $\sqrt{s} = 13$ TeV with the ATLAS detector*, [2411.02040](#).

- [115] Bijnens, Johan and Lönnblad, Leif and Sjöstrand, Torbjörn, “Theoretical Particle Physics Lecture Notes.” <http://home.thep.lu.se/~bijnens/fytn04/notes.pdf>.
- [116] J. Alwall, M. Herquet, F. Maltoni, O. Mattelaer and T. Stelzer, *MadGraph 5 : Going Beyond*, *JHEP* **06** (2011) 128 [[1106.0522](#)].
- [117] M. Bahr et al., *Herwig++ Physics and Manual*, *Eur. Phys. J.* **C58** (2008) 639 [[0803.0883](#)].
- [118] J. Bellm et al., *Herwig 7.1 Release Note*, [1705.06919](#).
- [119] S. Gieseke et al., *Herwig++ 2.5 Release Note*, [1102.1672](#).
- [120] K. Arnold et al., *Herwig++ 2.6 Release Note*, [1205.4902](#).
- [121] J. Bellm et al., *Herwig++ 2.7 Release Note*, [1310.6877](#).
- [122] J. Bellm et al., *Herwig 7.2 release note*, *Eur. Phys. J. C* **80** (2020) 452 [[1912.06509](#)].
- [123] G. Bewick et al., *Herwig 7.3 Release Note*, [2312.05175](#).
- [124] M. Cacciari, G.P. Salam and G. Soyez, *The anti- k_t jet clustering algorithm*, *JHEP* **04** (2008) 063 [[0802.1189](#)].
- [125] A. Papaefstathiou and G. White, *The electro-weak phase transition at colliders: confronting theoretical uncertainties and complementary channels*, *JHEP* **05** (2021) 099 [[2010.00597](#)].
- [126] CMS collaboration, *Combination of searches for Higgs boson pair production in proton-proton collisions at $\sqrt{s} = 13$ TeV*, *Phys. Rev. Lett.* **122** (2019) 121803 [[1811.09689](#)].
- [127] ATLAS collaboration, *Combination of searches for Higgs boson pairs in pp collisions at $\sqrt{s} = 13$ TeV with the ATLAS detector*, *Phys. Lett.* **B800** (2020) 135103 [[1906.02025](#)].
- [128] CMS collaboration, *Search for a new scalar resonance decaying to a pair of Z bosons in proton-proton collisions at $\sqrt{s} = 13$ TeV*, *JHEP* **06** (2018) 127 [[1804.01939](#)].
- [129] M. Cepeda et al., *Report from Working Group 2*, *CERN Yellow Rep. Monogr.* **7** (2019) 221 [[1902.00134](#)].
- [130] ATLAS collaboration, *Search for heavy resonances decaying into WW in the $e\nu\mu\nu$ final state in pp collisions at $\sqrt{s} = 13$ TeV with the ATLAS detector*, *Eur. Phys. J.* **C78** (2018) 24 [[1710.01123](#)].
- [131] ATLAS collaboration, *HL-LHC prospects for diboson resonance searches and electroweak vector boson scattering in the $WW/WZ \rightarrow l\nu qq$ final state*, Tech. Rep. [ATL-PHYS-PUB-2018-022](#), CERN, Geneva (Oct, 2018).
- [132] S.D. Lane, I.M. Lewis and M. Sullivan, *Resonant multiscalar production in the generic complex singlet model in the multi-TeV region*, *Phys. Rev. D* **110** (2024) 055017 [[2403.18003](#)].